Wld^S protein requires Nmnat activity and a short N-terminal sequence to protect axons in mice

Laura Conforti,[1] Anna Wilbrey,[1] Giacomo Morreale,[1] Lucie Janeckova,[1] Bogdan Beirowski,[1] Robert Adalbert,[1] Francesca Mazzola,[2] Michele Di Stefano,[2] Robert Hartley,[3] Elisabetta Babetto,[1] Trevor Smith,[1] Jonathan Gilley,[1] Richard A. Billington,[4,5] Armando A. Genazzani,[4,5] Richard R. Ribchester,[3] Giulio Magni,[2] and Michael Coleman[1]

[1]Babraham Institute, Babraham Research Campus, Cambridge CB22 3AT, England, UK
[2]Istituto di Biotecnologie Biochimiche, Università Politecnica delle Marche, 60131 Ancona, Italy
[3]Centre for Neuroscience Research, University of Edinburgh, Edinburgh EH8 9JZ, Scotland, UK
[4]Dipartimento di Scienze Chimiche, Alimentari, Farmaceutiche, e Farmacologiche and [5]Drug and Food Biotechnology Center, Università del Piemonte Orientale, 28100 Novara, Italy

The slow Wallerian degeneration (Wld^S) protein protects injured axons from degeneration. This unusual chimeric protein fuses a 70–amino acid N-terminal sequence from the Ube4b multiubiquitination factor with the nicotinamide adenine dinucleotide–synthesizing enzyme nicotinamide mononucleotide adenylyl transferase 1. The requirement for these components and the mechanism of Wld^S-mediated neuroprotection remain highly controversial. The Ube4b domain is necessary for the protective phenotype in mice, but precisely which sequence is essential and why are unclear. Binding to the AAA adenosine triphosphatase valosin-containing protein (VCP)/p97 is the only known biochemical property of the Ube4b domain. Using an in vivo approach, we show that removing the VCP-binding sequence abolishes axon protection. Replacing the Wld^S VCP-binding domain with an alternative ataxin-3–derived VCP-binding sequence restores its protective function. Enzyme-dead Wld^S is unable to delay Wallerian degeneration in mice. Thus, neither domain is effective without the function of the other. Wld^S requires both of its components to protect axons from degeneration.

Introduction

Axons are indispensable for neuronal function but degenerate early in nervous system disorders (Conforti et al., 2007a). Distal stumps of injured axons undergo Wallerian degeneration (Waller, 1850), a regulated, nonapoptotic death program that models disease processes (Coleman, 2005).

The slow Wallerian degeneration (*Wld^S*) gene dominantly delays Wallerian degeneration 10-fold (Mack et al., 2001; Ferri et al., 2003; Samsam et al., 2003; Coleman, 2005). *Wld^S* was identified by positional cloning (Coleman et al., 1998; Conforti et al., 2000) and replicates the protective phenotype in transgenic (Tg) mice (Mack et al., 2001), rats, and *Drosophila melanogaster* (Adalbert et al., 2005; Hoopfer et al., 2006; MacDonald et al., 2006). It fuses the N-terminal 70 amino acids (N70) of multiubiquitination factor Ube4b in frame to the NAD$^+$-synthesizing enzyme nicotinamide mononucleotide adenylyl transferase 1 (Nmnat1), separated by a short Wld18 linker sequence. The parent proteins are unchanged. Wld^S also delays axon degeneration in some diseases indicating similar mechanisms, particularly when axonal transport is blocked (Coleman, 2005).

Understanding how Wld^S protects axons should help exploit its therapeutic potential and reveal the degenerative mechanism. In this study, we address the protein domains required in vivo and their roles. Overexpressing Nmnat1 in Tg mice is not sufficient to protect axons (Conforti et al., 2007b), but in lentiviral-transduced primary culture, protection has been reported (Araki et al., 2004; Wang et al., 2005). Thus, the N-terminal 88 amino acids are required in vivo, and primary culture experiments do not replicate the protective mechanism fully. However, the specific necessary sequences and their roles remain unknown. Moreover, reports that Nmnat1 blocks other types of

Correspondence to Michael Coleman: michael.coleman@bbsrc.ac.uk

Abbreviations used in this paper: EMG, electromyography; FDB, flexor digitorum brevis; Nmnat, nicotinamide mononucleotide adenylyl transferase; SCG, spinal cervical ganglia; Tg, transgenic; VBM, VCP-binding motif; VCP, valosin-containing protein; Wld^S, slow Wallerian degeneration.

The Rockefeller University Press $30.00
J. Cell Biol. Vol. 184 No. 4 491–500
www.jcb.org/cgi/doi/10.1083/jcb.200807175

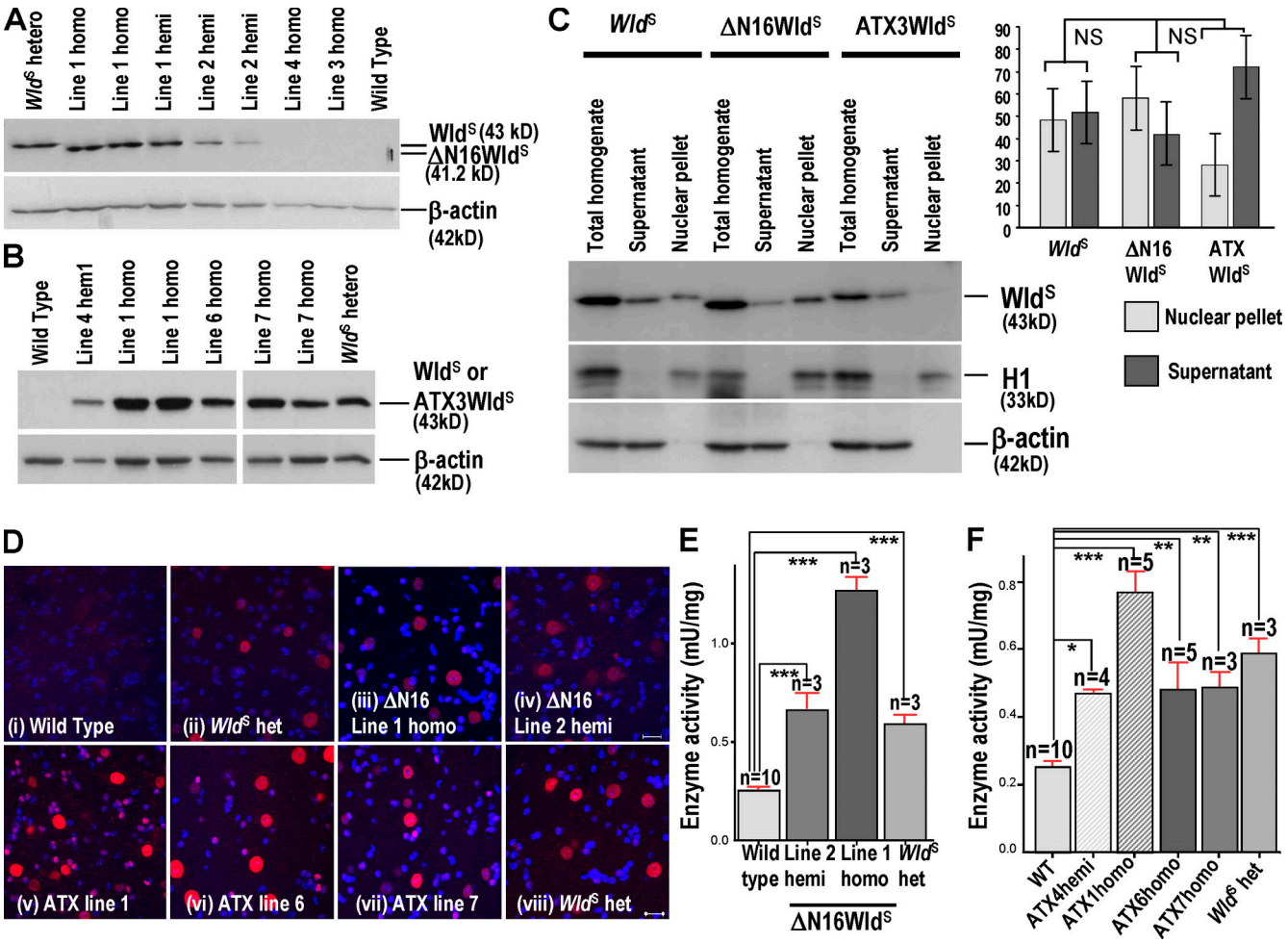

Figure 1. **Overexpression of ΔN16Wld^S and ATX3Wld^S in Tg mice.** (A and B) Western blots of ΔN16Wld^S and ATX3Wld^S brains probed with Wld18. ΔN16Wld^S lines 1 and 2 alone express a protein slightly smaller than Wld^S. The 43-kD ATX3Wld^S band matches that in *Wld^S*. (C) Brain Western blots of total homogenate and nuclear and cytoplasmic fractions of *Wld^S*, ΔN16Wld^S (line 1), and ATX3Wld^S (line 6). The graph shows integrated band intensities of nuclear and cytoplasmic fractions normalized to H1 and β-actin, respectively. These normalized figures were then expressed as a percentage of the total homogenate signal and normalized to the same respective markers (mean ± SD; $n = 3$). Statistical analysis was performed on the nuclear versus supernatant ratio using a Mann-Whitney test followed by a Bonferroni post-hoc test. (D) Immunofluorescence of lumbar spinal cord sections with Wld18 (red) and DAPI. Motor and interneuron nuclear signals in Tg ΔN16Wld^S (i–iv) and ATX3Wld^S (v–viii) show similar strength and distribution as *Wld^S* heterozygotes. Identical laser intensities and camera settings were used for each image. (E and F) Transgene products are enzymatically active. Nmnat activity is very significantly increased compared with wild-type (WT) brains in hemizygotes and homozygotes of all expressing Tg lines as well as *Wld^S* heterozygotes. Mean ± SD; *, $P < 0.05$; **, $P < 0.01$; ***, $P < 0.001$. Bars, 10 µm.

neurodegeneration in vivo without enzyme activity contrasts with primary culture data on axon degeneration, so a classical mammalian in vivo approach is needed to resolve this (Araki et al., 2004; Zhai et al., 2008).

N70 binds AAA ATPase valosin-containing protein (VCP) through a VCP-binding motif (VBM) in its N-terminal 16 amino acids (N16; Boeddrich et al., 2006; Morreale et al., 2009). In nuclei, in which Wld^S is most easily visualized, VCP influences local Wld^S targeting (Wilbrey et al., 2008). Recent data indicate that Wld^S can function in cytoplasm (Beirowski et al., 2009), in which VCP is extremely abundant. Thus, VCP interaction also likely affects local targeting of cytoplasmic Wld^S.

Early embryonic lethality precludes testing a role for VCP in null mice (Muller et al., 2007). Thus, we generated Tg mice expressing variant Wld^S with altered VCP-binding properties and lesioned their nerves. In view of the controversies over Nmnat activity, we also generated enzyme-dead Tg mice.

Results and discussion

Variant Wld^S Tg mice with an altered VCP-binding region

First, we tested the need for the VCP-binding sequence, expressing Wld^S without amino acids 2–16 in ΔN16Wld^S Tg mice (Fig. S1, available at http://www.jcb.org/cgi/content/full/jcb.200807175/DC1). Two of the four lines expressed protein on brain Western blots (Fig. 1 A; Samsam et al., 2003). Line 1 homozygotes expressed similar levels to *Wld^S* heterozygotes. Line 2 could not breed to homozygosity. Hemizygotes expressed slightly less, but still at a level where Wld^S delays axon degeneration significantly (Mack et al., 2001). Nmnat activity matched or exceeded that in Wld^S (Fig. 1 E), and lumbar spinal cord motor neurons, whose axons in the sciatic nerve we lesioned, express the protein (Fig. 1 D). The ΔN16Wld^S variant showed a clear cytoplasmic signal, with no significant difference in

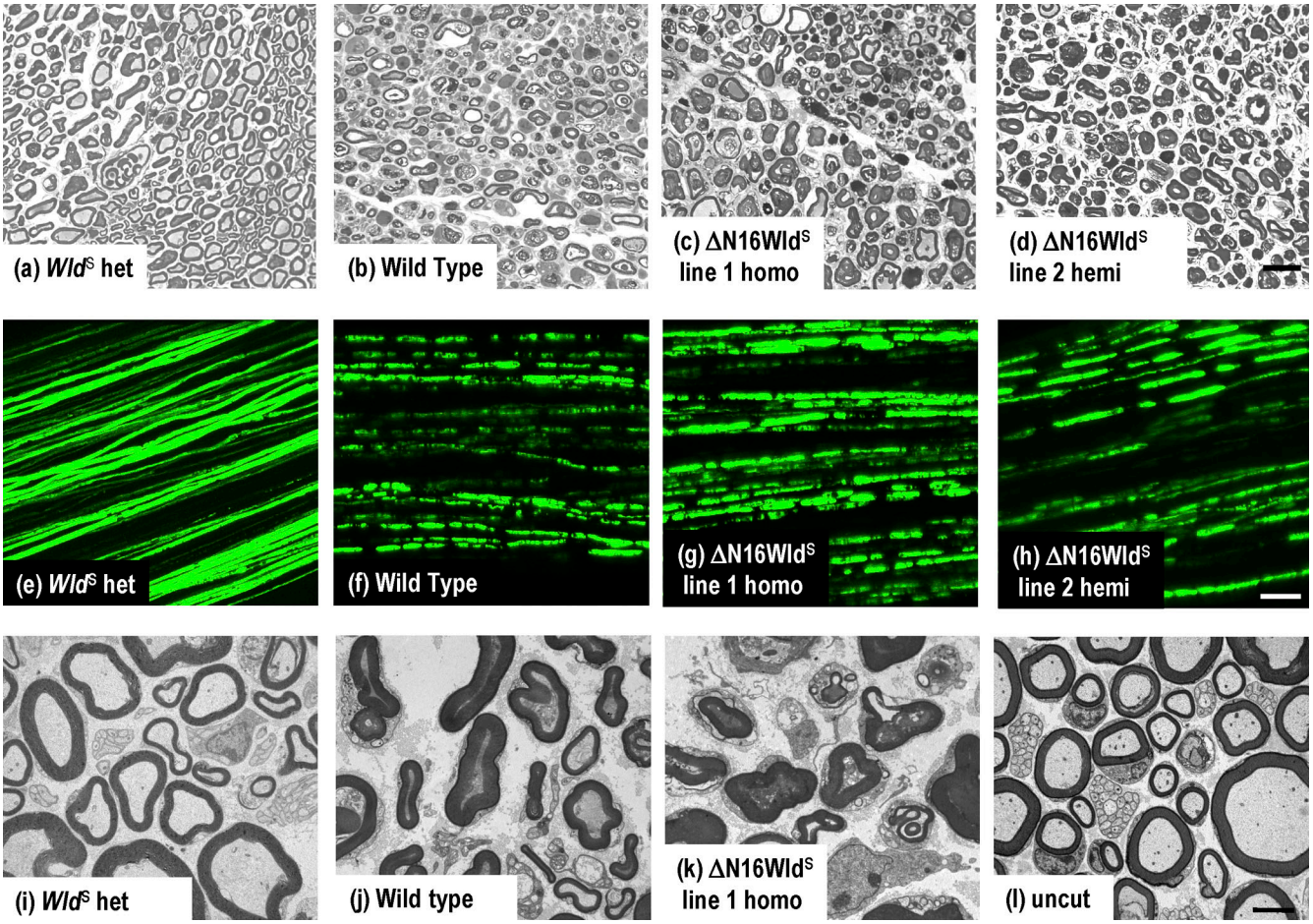

Figure 2. **Rapid Wallerian degeneration in ΔN16Wld^S Tg mice.** (a–d) Semithin sections of distal sciatic nerve 5 d after lesion. (a) Axons are well preserved in *Wld^S* heterozygotes, with intact myelin sheaths, uniform and regularly spaced cytoskeleton, and normal-shaped mitochondria. (b) Wild-type axons are degenerated, with collapsed myelin and disorganized or vacuolized cytoskeleton. (c and d) ΔN16Wld^S line 1 homozygous and line 2 hemizygous nerves are indistinguishable from wild type. (e–h) Tibial nerves from mice crossed to YFP-H show rapid loss of axon continuity in ΔN16Wld^S. (e) *Wld^S* heterozygotes 3 d after lesion show axon continuity. (f–h) In contrast, all lesioned wild-type and ΔN16Wld^S line 1 and line 2 axons lose continuity within 72 h. (i–l) Transmission electron microscopy of distal sciatic nerve 3 d after lesion. (i) Myelinated and unmyelinated axons are well preserved in *Wld^S* heterozygotes, which are indistinguishable from unlesioned nerves (l). (j) In wild type, myelin collapsed to form ovoids, the cytoskeleton is floccular or absent, and mitochondria are swollen or absent. (k) Nerves from ΔN16Wld^S line 1 homozygotes are indistinguishable from wild types. Bars: (a–d) 20 µm; (e–h) 50 µm; (i–l) 2 µm.

nuclear/cytoplasmic distribution relative to Wld^S at $n = 3$ (Fig. 1, C and D, i–iv).

We then replaced N16 with a 16–amino acid VCP-binding sequence from polyglutamine protein ataxin-3 (Atx-3; 277–291 plus start Met, ATX3) sharing only five residues (Fig. S1; Boeddrich et al., 2006). At least 5 of 12 lines expressed protein, and most experiments used line 1 and 6 homozygotes. Again, we confirmed protein expression and enzyme activity similar to or exceeding Wld^S heterozygotes (Fig. 1). Despite some variability, subcellular localization of ATX3Wld^S was not significantly different from Wld^S or ΔN16Wld^S ($n = 3$; Fig. 1 C), and the protein was in neuronal nuclei in the lumbar spinal cord (Fig. 1 D, v–vii).

Effect of the VCP-binding region on phenotype

5 d after sciatic nerve lesion, *Wld^S* heterozygotes retained 69.7 ± 1.8% of axons with normal cytoskeleton, unswollen mitochondria, and a regular myelin sheath of normal thickness compared with only 1.2 ± 0.4% in wild-type mice (Fig. 2 and Fig. S1). In contrast, ΔN16Wld^S was indistinguishable from wild type. Line 1 homozygotes and line 2 hemizygotes showed 2.3 ± 0.2% and 0.9 ± 0.2% surviving axons, respectively (Fig. 2, a–d; and Fig. S1). Axons lost continuity, as assessed by crossing to YFP-H Tg mice (Beirowski et al., 2004), by 3 d (Fig. 2, g and h), which is a low stringency test ruling out even a weak protective phenotype. Axons in *Wld^S* heterozygotes maintain continuity even at 5–14 d (Fig. 3). Finally, ultrastructural experiments confirmed that axons of ΔN16Wld^S mice retained little, if any, normal cytoskeleton and organelles after 3 d (Fig. 2, i–l). Thus, N16, which contains a VBM, is essential for Wld^S to delay Wallerian degeneration.

Replacing the VCP-binding site with the Atx-3 sequence restored strong axon protection similar to *Wld^S*. 5 d after nerve lesion, lines 1 and 6 showed highly significant structural preservation on semithin sections and retained axon continuity similar to *Wld^S* heterozygotes (Fig. 3 A and Fig. S1). Axons in other lines were also protected (Fig. S2, available at http://www.jcb.org/cgi/content/full/jcb.200807175/DC1).

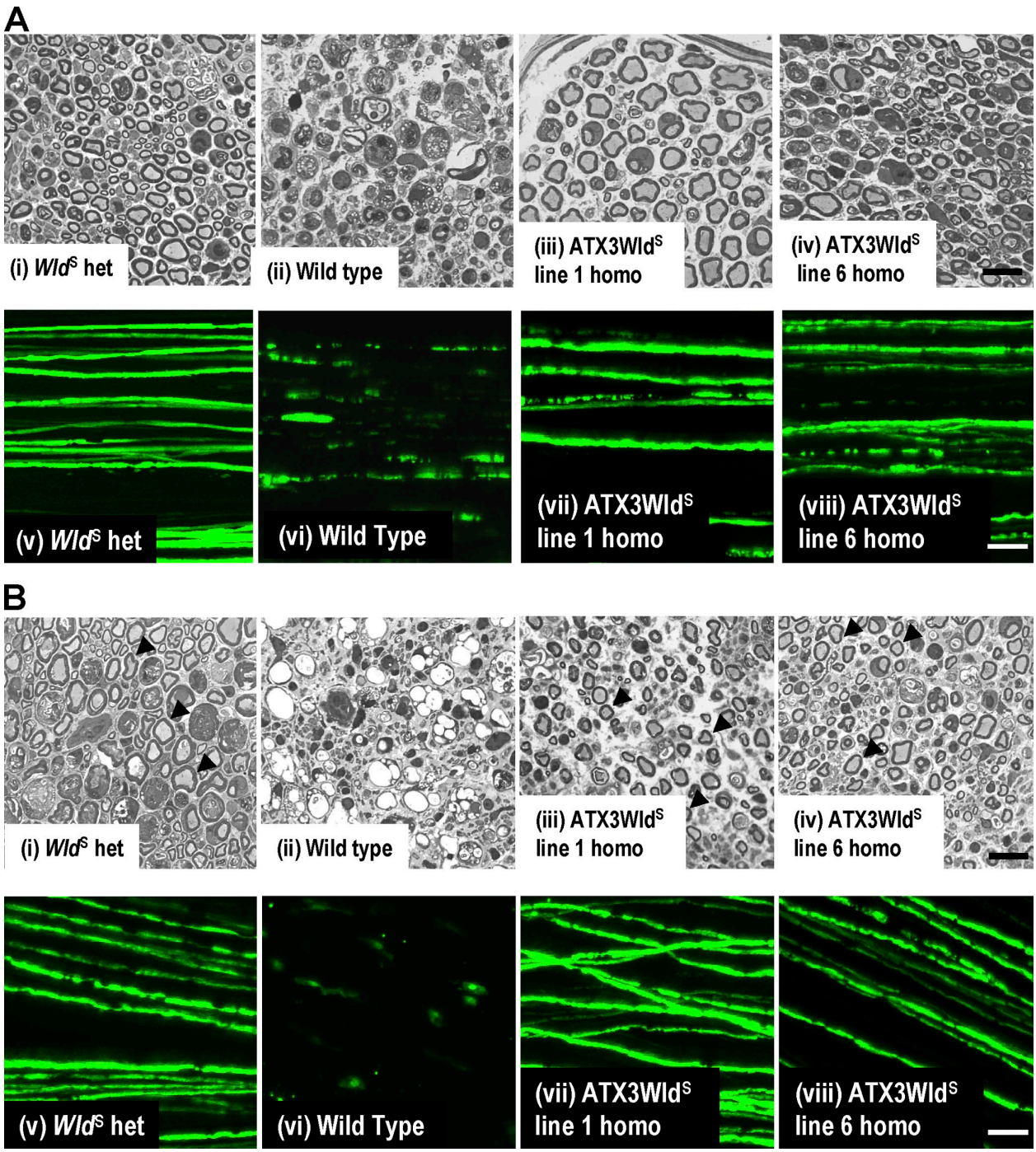

Figure 3. **ATX3Wld^S Tg mice show a Wld^S phenotype.** (A, i–iv) Semithin sections of distal sciatic nerve 5 d after lesion. (i and ii) Most axons are well preserved in *Wld^S* heterozygotes (i), but wild-type nerves (ii) are completely degenerated. (iii and iv) Nerves from ATX3Wld^S line 1 and line 6 show preservation similar to *Wld^S* heterozygotes. (v–viii) Confocal images of tibial nerve 5 d after sciatic lesion from mice crossed to YFP-H. (v) *Wld^S* heterozygotes maintain axon continuity. (vi) All wild-type axons are highly fragmented. (vii and viii) Many lesioned ATX3Wld^S axons maintain continuity. (B, i, iii, and iv) Semithin sections of distal sciatic nerve show preserved axons (arrowheads) 14 d after lesion in *Wld^S* heterozygotes (i) and ATX3Wld^S (iii and iv). (ii) Wild-type axons are completely degenerated and highly vacuolized. (v–viii) Confocal images of tibial nerves 14 d after sciatic nerve lesion in mice crossed to YFP-H. (v) *Wld^S* axons maintain continuity in contrast to the few remnants of the fragmented wild-type axons (vi). (vii and viii) Many axons in ATX3Wld^S were also continuous at this stringent time point. Bars: (i–iv) 20 µm; (v–viii) 50 µm.

We then applied more stringent tests to verify that ATX3-Wld^S mice have a full Wld^S phenotype. 14 d after sciatic lesion, distal axons on semithin sections were structurally preserved, as in *Wld^S* ($P > 0.05$). In whole-mount nerves, many YFP-H–labeled axons retained continuity (Fig. 3 B and Fig. S1). Little but debris remained in wild-type nerves. We then confirmed that lesioned axons and their neuromuscular synapses remained functional for at least 3 d. Evoked action potentials in tibial nerve/flexor digitorum brevis (FDB) preparations provoked robust contractile and electromyographic responses (Fig. 4 A and Video 1, available at

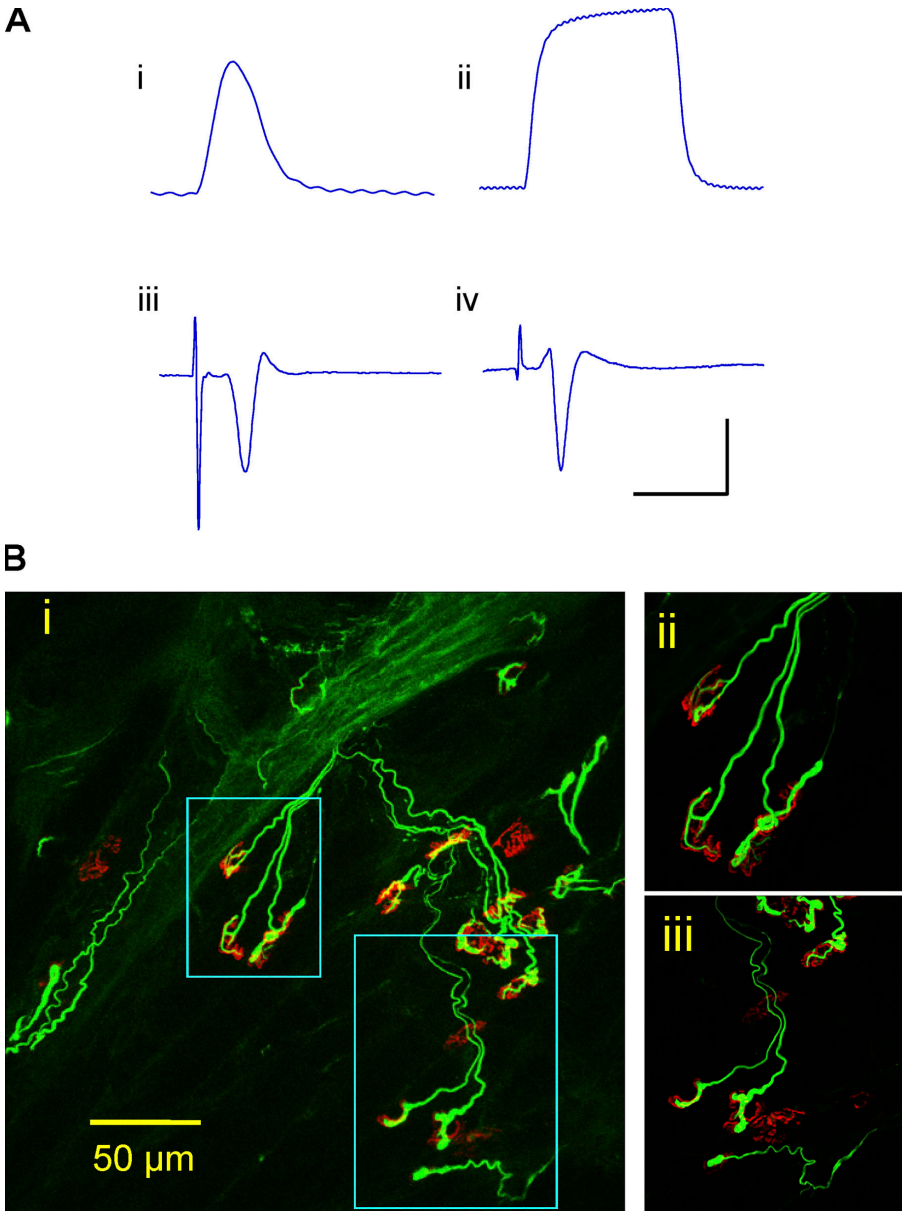

Figure 4. **Functional motor innervation.** (A) ATX3Wld^S mice show robust preservation of neuromuscular function 3 d after nerve lesion. (i and ii) Isometric single twitch (i) and 20-Hz tetanic tension (ii) responses of isolated FDB to tibial nerve stimulation. (iii and iv) Averaged (16 sweeps) extracellular evoked EMG responses to stimulation of 3-d axotomized FDB from ATX3Wld^S (iii) and *Wld^S* (iv). The x axis represents milliseconds, and the y axis represents millinewtons or microvolts. Bars: (i) 200 ms and 2 mN; (ii) 700 ms and 5 mN; (iii) 6 ms and 200 µV; (iv) 12 ms and 200 µV. (B) Confocal microscopy of axotomized FDB from an ATX3Wld^S line 5 mouse in which physiological recordings indicated robust preservation of neuromuscular function. Most motor endplates (TRITC–α-bungarotoxin staining; red) were innervated by neurofilament-positive axon collaterals and motor nerve terminals (green), but ∼20% of endplates were unoccupied. (i) Low power z-series projection. (ii and iii) Higher magnification images correspond to the boxed areas in panel i.

http://www.jcb.org/cgi/content/full/jcb.200807175/DC1) that were absent in controls (Video 2). Immunostaining for preserved presynaptic structures of 3-d axotomized neuromuscular junction showed most endplates partially or fully occupied by motor nerve terminals connected to intramuscular motor axons (Fig. 4 B).

We then treated spinal cervical ganglia (SCG) explants from these mice with vincristine to confirm these results using an assay in which axons are not cut (Ravula et al., 2007). As reported, Wld^S protected these axons (Wang et al., 2001; Conforti et al., 2007b). Consistent with our in vivo data, ΔN16Wld^S neurites degenerated at a wild-type rate, whereas ATX3Wld^S neurites remained largely intact 5 d after vincristine application (Fig. S2).

In summary, the Atx-3–derived VCP-binding sequence restores axon protective properties to ΔN16Wld^S that are indistinguishable from *Wld^S* in terms of structure, long-term survival, and axonal and synaptic function. Collectively, these results strongly support a role of the VBM in Wld^S-mediated axon protection.

Nmnat enzyme activity is required for the Wld^S phenotype

Having shown that N16 is necessary for the Wld^S phenotype in mice, we then tested the requirement for Nmnat activity in vivo and whether N16 and other N-terminal sequences, including Wld18, are sufficient. We made Tg mice expressing enzyme-dead Wld^S (W258A; Fig. S1) but retaining all N-terminal sequences.

Tg-expressing lines 2 and 4 showed no increase in brain Nmnat activity over wild type, whereas activity in *Wld^S* heterozygotes increased two- to threefold (Fig. 5, A and C). As before, we confirmed protein expression in motor neuron nuclei (Fig. 5 B) and we lesioned sciatic nerves. At the 3-d (low stringency) time point, homogeneous axoplasm and unswollen mitochondria could no longer be identified in semithin sections (Fig. 5 D, i and ii), and neither line retained axon continuity (Fig. 5 D, v and vi). The third expressing line showed similar wild-type–like behavior (unpublished data). In contrast, *Wld^S* heterozygous

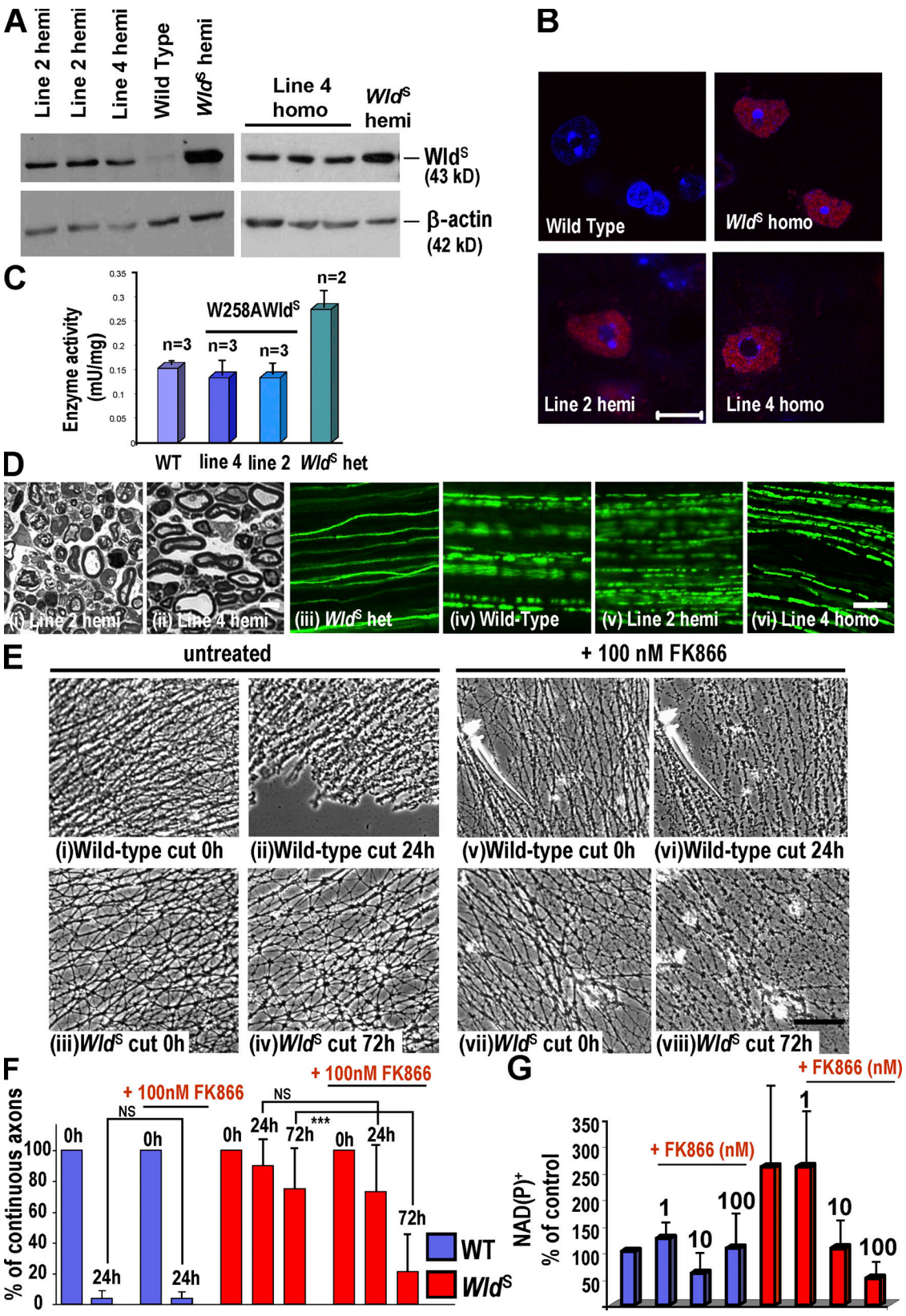

Figure 5. **Rapid Wallerian degeneration in W258AWld^S Tg mice.** (A) Brain Western blots from W258AWld^S Tg, *Wld^S*, and wild-type mice probed with Wld18. W258AWld^S lines 2 and 4 express a 43-kD band, which is absent in wild type. (B) Wld18 immunofluorescence (red) of lumbar spinal cord. Motor neuron nuclear signal strength and distribution in W258AWld^S lines match *Wld^S* heterozygotes. Identical laser intensities and camera settings were used for each image. (C) Nmnat1 activity is unaltered in the W258AWld^S brain. (D, i and ii) Semithin sections of W258AWld^S distal sciatic nerve 72 h after lesion. Axons are degenerated, similar to wild-type or ΔN16Wld^S axons (Fig 2). (iii–vi) In mice crossed to YFP-H, tibial nerve axons lose continuity within 72 h of sciatic lesion, except in Wld^S (iii). (E) SCG explants untreated (i–iv) or treated (v–viii) with 100 nM FK866 for 72 h and then cut. Unlike wild-type

mice expressing a similar level of Wld^S protein showed strong axon protection (Fig. 5 D, iii; and Fig. S1).

We confirmed rapid degeneration of injured W258AWld^S neurites in SCG explant cultures and added 1 mM exogenous NAD^+ either 24 or 0 h before cutting. As we previously found in wild-type neurites (Conforti et al., 2007b), neither treatment altered the rate of degeneration (Fig. S3 A, available at http://www.jcb.org/cgi/content/full/jcb.200807175/DC1). Although we cannot be sure how much NAD^+ entered the cells, these data are consistent with the notion that N16 and Nmnat activity must be physically linked in the same molecule to deliver Nmnat activity to a specific site. Thus, an intact VCP-binding region in N16 is not sufficient to confer any Wld^S phenotype in vivo without associated Nmnat activity, nor is N70 or even N70 + Wld18.

To test the causal link between NAD^+ production and axon protection, we then used FK866 to block the enzyme nicotinamide phosphoribosyltransferase. Nicotinamide phosphoribosyltransferase catalyzes the rate-limiting step for NAD^+ salvage from nicotinamide. FK866 strongly reduced NAD^+ or $NADP^+$ levels in Wld^S SCG cultures (Fig. 5 G), and this was accompanied by a modest, partial reversion of the phenotype. Very few morphologically normal neurites remained in FK866-treated Wld^S cultures 72 h after cutting (Fig. 5 E, vii and viii), whereas significantly more intact neurites remained in untreated Wld^S cultures (Fig. 5, E [iii and iv] and F). After 6 d, there remained an obvious, statistically significant difference (Fig. S3 B). These data suggest that NAD^+ synthesis is required for the Wld^S phenotype, but the incomplete reversion also suggests a need to consider other actions of Nmnat1 and/or other downstream metabolites. Alternatively, NAD^+ may be tightly regulated at specific loci in a way that the whole cell measurements do not reflect.

Finally, we tested whether Nmnat1 chaperone activity contributes to axon protection by Wld^S. Chaperone activity in the W258A mutant protein was similar to that reported for enzyme-dead Nmnat ($n = 3$; Zhai et al., 2008; and unpublished data), but as the mice show no axon protection, this is unlikely to be sufficient for the Wld^S phenotype.

By refining the N-terminal sequence needed for Wld^S protein to preserve injured axons in mice and showing that Nmnat enzyme activity is also required to protect axons in vivo, we conclude that Wld^S protects axons through a mechanism involving both of its parts. The absence of axon protection in ΔN16Wld^S mice confirms and extends our earlier data that Nmnat1 cannot substitute for Wld^S protein at a similar expression level (Conforti et al., 2007b). The accompanying paper shows that the two proteins are also not equivalent in *Drosophila* (see Avery et al. on p. 501 of this issue). However, Nmnat activity is required, and in Wld^S, it works together with the N-terminal VCP-binding sequence to protect axons. The function of N16 now holds essential clues as to where this enzyme activity is needed and why, and it will be interesting to find out whether other changes or additions to Nmnat1 can make it protective in vivo.

The only known biochemical property of N16 is binding VCP (Laser et al., 2006). The VBM is highly conserved among vertebrates and some invertebrates (Morreale et al., 2009), including *Drosophila*, which could help explain how murine Wld^S can function there through a mechanism involving VCP (Avery et al., 2009). At the cellular level, recent data indicate that Wld^S can function outside nuclei (Beirowski et al., 2009), so we tested whether N16 binding to VCP (which is abundant in the cytoplasm as well as the nucleus) tethers some Wld^S in the cytoplasm. ΔN16 variant is abundant in cytoplasm (Fig. 1 C), indicating that the functional importance of N16 is not solely to retain the protein in the cytoplasm. Instead, we propose a finer targeting role. As N16 binding to VCP influences local targeting of Wld^S within nuclei (Wilbrey et al., 2008), it likely has a similar local effect in cytoplasm. Thus, the critical function of N16 may be local targeting of Nmnat1 to a cytoplasmic site where it is needed for axon protection.

Such a model may explain why overexpressing wild-type Nmnat1 without N16 fails to produce any Wld^S phenotype in Tg mice (Conforti et al., 2007b), whereas overexpression in lentiviral-transduced cultures or in *Drosophila* does reproduce the phenotype to some extent (Araki et al., 2004; Hoopfer et al., 2006; MacDonald et al., 2006). In higher expressing systems with shorter axons, Nmnat1 may reach levels at which focal targeting becomes unnecessary. However, high Nmnat1 expression levels could also trigger unrelated mechanisms.

The local targeting model raises two important questions: what is the critical site, and what does Nmnat1 do there? A local bioenergetics mechanism for NAD^+ within mitochondria has been proposed (Wang et al., 2005). However, the ability of Wld^S to maintain axonal NAD^+ and ATP levels could be an effect of axon survival rather than a cause, and how VCP binding and N16 fit such a model is not clear. Further investigations of VCP in mitochondria could shed light on this issue (Braun et al., 2006). An alternative location that does connect VCP and NAD^+ is the ER. VCP is particularly abundant here (Ye et al., 2005), and NAD^+ is a key upstream regulator of calcium signaling in this organelle through enzymes such as CD38 (Macgregor et al., 2007).

NAD^+ is also a substrate for the sirtuin family of histone deacetylases (Yang and Sauve, 2006) and for the ADP ribosylase PARP-1 (Kim et al., 2005), and Nmnat protects against reactive oxygen species (Press and Milbrandt, 2008). A Sirt1-mediated mechanism (Araki et al., 2004) is not supported by subsequent data (Wang et al., 2005; Conforti et al., 2007b; Avery et al., 2009), but these other possibilities remain plausible. However, a chaperone-mediated mechanism for axon protection (Zhai et al., 2008) is not supported by our data.

Other functions of VCP include roles in the cell cycle, homotypic membrane fusion, nuclear envelope reconstruction, postmitotic Golgi reassembly, DNA damage response, suppression of apoptosis, ER-associated protein degradation, and ubiquitin-dependent protein degradation (Watts et al., 2004). Thus, if the critical function of N16 is binding to VCP, one or more of these sites

axons (i, ii, v, and vi), untreated Wld^S axons are intact 72 h after being cut (iv) but when treated with FK866 are more degenerated (viii). (F) Quantification of continuous neurites (or neurite bundles). ***, $P < 0.0001$ (one-way analysis of variance followed by Bonferroni post-hoc test); $n = 8$ (wild type [WT]) and 9 (*Wld*^{S}). (G) NAD^+ or $NADP^+$ levels in wild-type and Wld^S explants ± FK866 at 1–100 nM. Mean of three different experiments. (C, F, and G) Mean ± SD. Bars: (B, D, i and ii, and E) 10 µm; (D, iii–vi) 100 µm.

could be important. VCP also has many associations with neurodegenerative disease as a component of intranuclear and cytoplasmic aggregates (Kobayashi et al., 2007), as the mutated gene in the rare neurological disorder inclusion body myopathy associated with Paget disease of bone and frontotemporal dementia (Watts et al., 2004), and through binding to Atx-3 and other polyglutamine proteins (Hirabayashi et al., 2001; Boeddrich et al., 2006).

As there are no null or conditional null VCP mice, VCP-independent mechanisms cannot be tested further using in vivo mouse experiments. We cannot rule out a role for other amino acids in common between the Atx-3–derived VCP-binding sequence and N16 or an influence on Wld^S turnover. However, in *Drosophila*, where targeted RNAi in specific neurons overcomes lethality, VCP knockdown significantly weakens the Wld^S phenotype (Avery et al., 2009). Collectively, these data strongly suggest that VCP binding is the critical property of this sequence that is required for the phenotype.

Like other chimeric proteins, Wld^S has a biological activity that requires both of its parts. In other cases, this can be the result of a conformational change that confers a new property such as affinity for a different receptor in the case of a ligand (Campbell et al., 1997). The combination of two different proteins to form a chimera often arises from chromosome translocations or gene duplications and has evolutionary relevance. Wld^S arose in the laboratory mouse, so it is not the result of generations of adaptive mutations. Nevertheless, this is another intriguing example of how protein domains can be combined to produce a completely new function.

The impressive correlation between the phenotypes of *Wld*^{S} mice, rats, and *Drosophila*, each carrying the mouse cDNA, indicates that the degenerative pathway that it blocks is well conserved in evolution. Even in *Drosophila*, Nmnat1 cannot fully substitute for Wld^S in conferring axon protection, although a weak effect can be obtained from Nmnat1 overexpression alone, maybe reflecting higher expression levels reached in the fly with the use of a different promoter (MacDonald et al., 2006; Avery et al., 2009). VCP-binding sequences are required for the full Wld^S phenotype in *Drosophila* as well as in mice, and down-regulation of ter94, the *Drosophila* homologue of VCP, significantly weakens the phenotype (Avery et al., 2009). These similarities validate *Drosophila* as a model to study axon degeneration and protection by Wld^S and demonstrate how *Drosophila* experiments can provide information not easily obtainable in the mouse.

In summary, we show that N16, which contains a VBM, is necessary for Wld^S to delay Wallerian degeneration, and this sequence acts together with Nmnat1 activity. In this study, we propose a new model for Wld^S action that explains the requirement of both N-terminal Ube4b-derived sequence and Nmnat1 enzyme activity. Having strongly implicated VCP binding in the protective mechanism and having shown that VCP binding helps direct the subcellular distribution of Wld^S, we suggest that the role of the N-terminal region is to deliver Nmnat activity to an important, specific subcellular site. Further studies are necessary to identify this specific site and to understand what Nmnat1 does there to produce the Wld^S phenotype.

Materials and methods

Generation of Tg mice

The ΔN16Wld^S Tg construct was generated as previously reported (Mack et al., 2001; Conforti et al., 2007b) using the forward PCR primer 5′-TAGCCCAAGCTTTAGAGGAAAGCGATGCTTGCTGGTGGACAGACCTC-3′ (5′ HindIII tag and start codon underlined). For the ATX3Wld^S construct, the primer 5′-AGCCCAAGCTTTAGAGGAAAGCGATG**ACTTCAGAAGAGCTTCGGAAGAGACGAGAAGCCTACTTGAAAAA*CTTGCTGGTGGACAGACCT***-3′ (5′ HindIII tag and start codon underlined, Atx-3 sequences in bold, and Wld^S sequences in bold and italic) and its reverse complement were annealed and mixed with linearized ΔN16Wld^S. The mix was used as a template for PCR with the reverse primer that has been previously described (Mack et al., 2001; Conforti et al., 2007b) and the forward primer 5′-AGCCCAAGCTTTAGAGGAAAGCGATGACTTC-3′ (5′ HindIII tag and start codon underlined). For the W258AWld^S construct, tryptophan 258 of Wld^S was mutated to an alanine using the QuikChange Site-Directed Mutagenesis kit (Agilent Technologies) with the primer 5′-GCGTGCCCAACTTGGCGAAGATGGAGGAC-3′ and its reverse complementary primer (W→A mutation underlined).

Pronuclear injection of the EcoRI–NdeI fragments (Fig. S1) into an F1 C57BL-CBA strain was performed by the in-house Gene Targeting Facility. Animal work was performed in accordance with the 1986 Animals (Scientific Procedures) Act under project licence PPL 80/1778.

Genotyping

Tg mice were identified by Southern blotting as described previously (Conforti et al., 2007b). YFP-H mice (Feng et al., 2000) were obtained from The Jackson Laboratory and genotyped by Southern blotting (YFP probe generated by PCR from YFP-H mouse genomic DNA using the primers 5′-CGAACTCCAGCAGGACCATGTGAT-3′ and 5′-CTTCTTCAAGGACGACGGCAACTACAAG-3′).

Western blotting and Nmnat enzyme activity assay

Western blotting and Nmnat enzyme activity assays of sagittally divided half brains were performed as described previously (Conforti et al., 2007b). Subcellular fractionation of the nuclear and cytoplasmic compartments was performed as described previously (Beirowski et al., 2009). For these experiments, *Wld*^{S} heterozygotes, ΔN16Wld^S line 1, and ATX3Wld^S line 6 mice were used. In addition to Wld18 (1:2,000), mouse monoclonal anti–histone H1 (1:500; Millipore) and mouse monoclonal anti–β-actin (1:5,000; Abcam) were used as loading controls for the nuclear and the cytoplasmic fraction, respectively. All subcellular pellets were resuspended in the same volume as the starting total homogenate. Identical volumes of each fraction were loaded on the gels. For quantification, Western blot band intensities were determined with ImageJ software (National Institutes of Health) and analyzed as described in the figure legends.

Statistical analysis was performed using one-way analysis of variance followed by Dunnett's *t* post-hoc test or, when this was not applicable, by Kruskall-Wallis analysis followed by Mann-Whitney tests.

Immunocytochemistry

20-µm cryostat lumbar spinal cord sections of 4% paraformaldehyde perfusion-fixed mice were immunostained for Wld18 and imaged as described previously (Conforti et al., 2007b). Isolated FDB muscles were whole-mount immunostained for neurofilament and/or SV2, and acetylcholine receptors at motor endplates were counterstained with TRITC–α-bungarotoxin and imaged as described previously (Gillingwater et al., 2002).

Acquisition and processing of images

Bright field images were acquired on a microscope (IX8I; Olympus) coupled to a digital camera (U-TV 0.5XC; Olympus) using AnalySIS software (Soft Imaging System, GmbH). The objectives used were UPlanFI 4× NA 0.13, UPLanFI 10× NA 0.3, LCPlanFI 20× NA 0.40 (all air objectives), and UPLanSApo oil immersion 100× NA 1.40. Confocal fluorescent images were acquired using a confocal microscope system (LSM 510 Meta; Carl Zeiss, Inc.) built around an Axiovert 200 (Carl Zeiss, Inc.), and z series were merged using algorithms from LSM Software Release 3.2 (Carl Zeiss, Inc.). For colocalization analysis, the multitrack configuration mode was applied to avoid signal cross talk between individual fluorophores. The objectives used were Plan-Neofluar 20× NA 0.5 and oil immersion Plan-Apochromat 63× NA 1.4. Tissue preparations were mounted in Vectashield medium (Vector Laboratories). The fluorophores used were YFP

and Alexa Fluor 568. Nuclei were stained with DAPI. All images were acquired at room temperature.

Nerve lesion

Mice were anaesthetized with a mixture of 100 mg/kg ketamine (Fort Dodge Animal Health) and 5 mg/kg xylazine (Pfizer). Right sciatic nerves were transected at the upper thigh, and mice were killed by cervical dislocation 72 h to 14 d later. The swollen first 2 mm of distal nerve was discarded, and the remaining sciatic nerve stump was used for light and electron microscopy (see following section). For YFP-H mice, the tibial nerve was removed for confocal microscopy.

Light and electron microscopy

Nerves were fixed for at least 24 h in 0.1 M of phosphate buffer containing 4% paraformaldehyde and 2.5% glutardialdehyde, embedded in Durcupan resin (Fluka), and processed for light and electron microscopy as previously described (Beirowski et al., 2004).

Electrophysiology

Mice were killed by cervical dislocation. Isometric tension recordings and electromyography (EMG) were performed as described previously (Barry and Ribchester, 1995; Costanzo et al., 1999). Tibial nerve/FDB preparations were dissected, pinned to a Sylgard-lined dish, bathed in oxygenated mammalian physiological saline (137 mM Na^+, 4 mM K^+, 2 mM Ca^{2+}, 1 mM Mg^{2+}, 147 mM Cl, 5 mM glucose, and 5 mM Hepes, pH 7.2–7.4, equilibrated with 100% oxygen), connected either to a sensitive force transducer via their tendons or to a pair of stainless steel wires insulated within 500 µm of their tips, and inserted into the belly of the isolated muscle. The tibial nerve was stimulated using a suction electrode and tension, or EMG recordings were made on a laptop computer (Macintosh G4; Apple) using Chart version 4.1.1 (ADInstruments Ltd.) and Scope version 3.6.8 (ADInstruments Ltd.) software via a Powerlab 4/20T interface (ADInstruments Ltd.). Nerves were stimulated using 50–200-µs pulses, with 0.1–1-mA intensity at 1–20 Hz either from the Powerlab unit or using an isolated pulse stimulator (model 210; A-M Systems) supplying variable 1–10-V pulses for 200 µs in duration and at frequencies of 1–40 Hz. In some experiments, muscle contractions were also recorded as short videos through a dissecting microscope (Wild M5A; Spectra Services) using a digital camera (Coolpix 4500; Nikon).

Analysis of YFP-labeled nerves

Sciatic and tibial nerves were quickly removed from humanely killed mice, processed, and imaged as described previously (Conforti et al., 2007b).

SCG explant cultures and NAD^+ or $NADP^+$ assay

SCG explants were dissected, cultured, and lesioned as previously described (Buckmaster et al., 1995). Neurites were allowed to extend for 7 d in all cultures before any treatment. In vincristine experiments, this was used at a 0.02-µM final concentration, and the day of treatment was considered time 0. In experiments with FK866, the appropriate concentration was applied, and the cultures were kept for 72 h in the presence of the drug. At this time, some of the explants were collected in 100 ml H_2O for NAD^+ or $NADP^+$ determination as described in Billington et al. (2008). Other explants were cut, and the degeneration of the distal axons followed for another 72 h.

Online supplemental material

Fig. S1 shows the constructs used to generate Tg mice and the quantification of axon survival. Fig. S2 shows the survival of ATX3Wld^S and ΔN16Wld^S axons in vivo and in vitro. Fig. S3 shows the effects of increasing and decreasing NAD^+. Videos 1 and 2 show the contraction of stimulated ATX3Wld^S and wild-type FDB muscle, respectively, 3 d after sciatic nerve lesion. Online supplemental material is available at http://www.jcb.org/cgi/content/full/jcb.200807175/DC1.

We thank Dr. Anne Segonds-Pichon for statistical advice and Dr. Marc Freeman for helpful discussion and for sharing unpublished data.

This work was funded by the Biotechnology and Biological Sciences Research Council, Medical Research Council, and a Royal Society of Edinburgh/Scottish Executive Support Research Fellowship held by R.R. Ribchester during this study.

Submitted: 31 July 2008
Accepted: 21 January 2009

References

Adalbert, R., T.H. Gillingwater, J.E. Haley, K. Bridge, B. Beirowski, L. Berek, D. Wagner, D. Grumme, D. Thomson, A. Celik, et al. 2005. A rat model of slow Wallerian degeneration (WldS) with improved preservation of neuromuscular synapses. *Eur. J. Neurosci.* 21:271–277.

Araki, T., Y. Sasaki, and J. Milbrandt. 2004. Increased nuclear NAD biosynthesis and SIRT1 activation prevent axonal degeneration. *Science*. 305:1010–1013.

Avery, M.A., A. Sheehan, K.S. Kerr, J. Wang, and M. Freeman. 2009. Wld^S requires Nmnat1 enzymatic activity and N16–VCP interactions to suppress Wallerian degeneration. *J. Cell Biol.* 184:501–513.

Barry, J.A., and R.R. Ribchester. 1995. Persistent polyneuronal innervation in partially denervated rat muscle after reinnervation and recovery from prolonged nerve conduction block. *J. Neurosci.* 15:6327–6339.

Beirowski, B., L. Berek, R. Adalbert, D. Wagner, D.S. Grumme, K. Addicks, R.R. Ribchester, and M.P. Coleman. 2004. Quantitative and qualitative analysis of Wallerian degeneration using restricted axonal labelling in YFP-H mice. *J. Neurosci. Methods*. 134:23–35.

Beirowski, B., E. Babetto, J. Gilley, F. Mazzola, L. Conforti, L. Janeckova, G. Magni, R.R. Ribchester, and M.P. Coleman. 2009. Non-nuclear Wld^S determines its neuroprotective efficacy for axons and synapses in vivo. *J. Neurosci.* 29:653–668.

Billington, R.A., C. Travelli, E. Ercolano, U. Galli, C.B. Roman, A.A. Grolla, P.L. Canonico, F. Condorelli, and A.A. Genazzani. 2008. Characterization of NAD uptake in mammalian cells. *J. Biol. Chem.* 283:6367–6374.

Boeddrich, A., S. Gaumer, A. Haacke, N. Tzvetkov, M. Albrecht, B.O. Evert, E.C. Muller, R. Lurz, P. Breuer, N. Schugardt, et al. 2006. An arginine/lysine-rich motif is crucial for VCP/p97-mediated modulation of ataxin-3 fibrillogenesis. *EMBO J.* 25:1547–1558.

Braun, R.J., H. Zischka, F. Madeo, T. Eisenberg, S. Wissing, S. Buttner, S.M. Engelhardt, D. Buringer, and M. Ueffing. 2006. Crucial mitochondrial impairment upon CDC48 mutation in apoptotic yeast. *J. Biol. Chem.* 281:25757–25767.

Buckmaster, E.A., V.H. Perry, and M.C. Brown. 1995. The rate of Wallerian degeneration in cultured neurons from wild-type and C57bl/Wld(S) mice depends on time in culture and may be extended in the presence of elevated K+ levels. *Eur. J. Neurosci.* 7:1596–1602.

Campbell, R.K., E.R. Bergert, Y. Wang, J.C. Morris, and W.R. Moyle. 1997. Chimeric proteins can exceed the sum of their parts: implications for evolution and protein design. *Nat. Biotechnol.* 15:439–443.

Coleman, M. 2005. Axon degeneration mechanisms: commonality amid diversity. *Nat. Rev. Neurosci.* 6:889–898.

Coleman, M.P., L. Conforti, E.A. Buckmaster, A. Tarlton, R.M. Ewing, M.C. Brown, M.F. Lyon, and V.H. Perry. 1998. An 85-kb tandem triplication in the slow Wallerian degeneration (Wlds) mouse. *Proc. Natl. Acad. Sci. USA*. 95:9985–9990.

Conforti, L., A. Tarlton, T.G. Mack, W. Mi, E.A. Buckmaster, D. Wagner, V.H. Perry, and M.P. Coleman. 2000. A Ufd2/D4Cole1e chimeric protein and overexpression of Rbp7 in the slow Wallerian degeneration (WldS) mouse. *Proc. Natl. Acad. Sci. USA*. 97:11377–11382.

Conforti, L., R. Adalbert, and M.P. Coleman. 2007a. Neuronal death: where does the end begin? *Trends Neurosci.* 30:159–166.

Conforti, L., G. Fang, B. Beirowski, M.S. Wang, L. Sorci, S. Asress, R. Adalbert, A. Silva, K. Bridge, X.P. Huang, et al. 2007b. NAD(+) and axon degeneration revisited: Nmnat1 cannot substitute for Wld(S) to delay Wallerian degeneration. *Cell Death Differ.* 14:116–127.

Costanzo, E.M., J.A. Barry, and R.R. Ribchester. 1999. Co-regulation of synaptic efficacy at stable polyneuronally innervated neuromuscular junctions in reinnervated rat muscle. *J. Physiol.* 521:365–374.

Feng, G., R.H. Mellor, M. Bernstein, C. Keller-Peck, Q.T. Nguyen, M. Wallace, J.M. Nerbonne, J.W. Lichtman, and J.R. Sanes. 2000. Imaging neuronal subsets in transgenic mice expressing multiple spectral variants of GFP. *Neuron*. 28:41–51.

Ferri, A., J.R. Sanes, M.P. Coleman, J.M. Cunningham, and A.C. Kato. 2003. Inhibiting axon degeneration and synapse loss attenuates apoptosis and disease progression in a mouse model of motoneuron disease. *Curr. Biol.* 13:669–673.

Gillingwater, T.H., D. Thomson, T.G. Mack, E.M. Soffin, R.J. Mattison, M.P. Coleman, and R.R. Ribchester. 2002. Age-dependent synapse withdrawal at axotomised neuromuscular junctions in Wld(s) mutant and Ube4b/Nmnat transgenic mice. *J. Physiol.* 543:739–755.

Hirabayashi, M., K. Inoue, K. Tanaka, K. Nakadate, Y. Ohsawa, Y. Kamei, A.H. Popiel, A. Sinohara, A. Iwamatsu, Y. Kimura, et al. 2001. VCP/p97 in abnormal protein aggregates, cytoplasmic vacuoles, and cell death, phenotypes relevant to neurodegeneration. *Cell Death Differ.* 8:977–984.

Hoopfer, E.D., T. McLaughlin, R.J. Watts, O. Schuldiner, D.D. O'Leary, and L. Luo. 2006. Wlds protection distinguishes axon degeneration following injury from naturally occurring developmental pruning. *Neuron*. 50:883–895.

Kim, M.Y., T. Zhang, and W.L. Kraus. 2005. Poly(ADP-ribosyl)ation by PARP-1: 'PAR-laying' NAD+ into a nuclear signal. *Genes Dev.* 19:1951–1967.

Kobayashi, T., A. Manno, and A. Kakizuka. 2007. Involvement of valosin-containing protein (VCP)/p97 in the formation and clearance of abnormal protein aggregates. *Genes Cells*. 12:889–901.

Laser, H., L. Conforti, G. Morreale, T.G. Mack, M. Heyer, J.E. Haley, T.M. Wishart, B. Beirowski, S.A. Walker, G. Haase, et al. 2006. The slow Wallerian degeneration protein, WldS, binds directly to VCP/p97 and partially redistributes it within the nucleus. *Mol. Biol. Cell*. 17:1075–1084.

MacDonald, J.M., M.G. Beach, E. Porpiglia, A.E. Sheehan, R.J. Watts, and M.R. Freeman. 2006. The *Drosophila* cell corpse engulfment receptor Draper mediates glial clearance of severed axons. *Neuron*. 50:869–881.

Macgregor, A.T., S. Rakovic, A. Galione, and D.A. Terrar. 2007. Dual effects of cyclic ADP-ribose on sarcoplasmic reticulum Ca2+ release and storage in cardiac myocytes isolated from guinea-pig and rat ventricle. *Cell Calcium*. 41:537–546.

Mack, T.G., M. Reiner, B. Beirowski, W. Mi, M. Emanuelli, D. Wagner, D. Thomson, T. Gillingwater, F. Court, L. Conforti, et al. 2001. Wallerian degeneration of injured axons and synapses is delayed by a Ube4b/Nmnat chimeric gene. *Nat. Neurosci.* 4:1199–1206.

Morreale, G., L. Conforti, J. Coadwell, A.L. Wilbrey, and M.P. Coleman. 2009. Evolutionary divergence of valosin-containing protein/cell division cycle protein 48 binding interactions among endoplasmic reticulum-associated degradation proteins. *FEBS J.* doi:10.1111/j.1742-4658.2008.06858.x.

Muller, J.M., K. Deinhardt, I. Rosewell, G. Warren, and D.T. Shima. 2007. Targeted deletion of p97 (VCP/CDC48) in mouse results in early embryonic lethality. *Biochem. Biophys. Res. Commun.* 354:459–465.

Press, C., and J. Milbrandt. 2008. Nmnat delays axonal degeneration caused by mitochondrial and oxidative stress. *J. Neurosci.* 28:4861–4871.

Ravula, S.K., M.S. Wang, M.A. McClain, S.A. Asress, B. Frazier, and J.D. Glass. 2007. Spatiotemporal localization of injury potentials in DRG neurons during vincristine-induced axonal degeneration. *Neurosci. Lett.* 415:34–39.

Samsam, M., W. Mi, C. Wessig, J. Zielasek, K.V. Toyka, M.P. Coleman, and R. Martini. 2003. The Wlds mutation delays robust loss of motor and sensory axons in a genetic model for myelin-related axonopathy. *J. Neurosci.* 23:2833–2839.

Waller, A. 1850. Experiments on the section of glossopharyngeal and hypoglossal nerves of the frog, and observations of the alternatives produced thereby in the structure of their primitive fibres. *Philos. Trans. R. Soc. Lond. (1776–1886)*. 140:423–429.

Wang, J., Q. Zhai, Y. Chen, E. Lin, W. Gu, M.W. McBurney, and Z. He. 2005. A local mechanism mediates NAD-dependent protection of axon degeneration. *J. Cell Biol.* 170:349–355.

Wang, M.S., G.F. Fang, D.G. Culver, A.A. Davis, M.M. Rich, and J.D. Glass. 2001. The Wld(S) protein protects against axonal degeneration: a model of gene therapy for peripheral neuropathy. *Ann. Neurol.* 50:773–779.

Watts, G.D., J. Wymer, M.J. Kovach, S.G. Mehta, S. Mumm, D. Darvish, A. Pestronk, M.P. Whyte, and V.E. Kimonis. 2004. Inclusion body myopathy associated with Paget disease of bone and frontotemporal dementia is caused by mutant valosin-containing protein. *Nat. Genet.* 36:377–381.

Wilbrey, A.L., J.E. Haley, T.M. Wishart, L. Conforti, G. Morreale, B. Beirowski, E. Babetto, R. Adalbert, T.H. Gillingwater, T. Smith, et al. 2008. VCP binding influences intracellular distribution of the slow Wallerian degeneration protein, Wld(S). *Mol. Cell. Neurosci.* 38:325–340.

Yang, T., and A.A. Sauve. 2006. NAD metabolism and sirtuins: metabolic regulation of protein deacetylation in stress and toxicity. *AAPS J.* 8:E632–E643.

Ye, Y., Y. Shibata, M. Kikkert, S. van Voorden, E. Wiertz, and T.A. Rapoport. 2005. Inaugural Article: Recruitment of the p97 ATPase and ubiquitin ligases to the site of retrotranslocation at the endoplasmic reticulum membrane. *Proc. Natl. Acad. Sci. USA*. 102:14132–14138.

Zhai, R.G., F. Zhang, P.R. Hiesinger, Y. Cao, C.M. Haueter, and H.J. Bellen. 2008. NAD synthase NMNAT acts as a chaperone to protect against neurodegeneration. *Nature*. 452:887–891.